Reversible Hydrogenation of Surface N Atoms To Form NH on Pt(111)

Eldad Herceg, Kumudu Mudiyanselage, and Michael Trenary*

Department of Chemistry, University of Illinois at Chicago, 845 West Taylor Street, Chicago, Illinois 60607-7061

Received: July 13, 2004; In Final Form: December 6, 2004

The formation and dissociation chemistry of the NH species on Pt(111) was characterized with reflection absorption infrared spectroscopy and temperature programmed desorption. Irradiation of a chemisorbed bilayer of ammonia with a 100 eV electron beam at 85 K leads to a mixture of NH, N, and H on the surface. Annealing to temperatures in the range of 200−300 K leads to reaction of N and H to form additional NH. The NH species has an intense and narrow NH stretch peak at 3320 cm^{-1}, while no peak due to the PtNH bend is observed above 800 cm^{-1}. The NH species is stable up to a temperature of ∼400 K. The surface N atoms produced from NH dissociation are readily hydrogenated back to NH by exposure of the surface to H_2. However, NH cannot be further hydrogenated to generate adsorbed NH_2 or to NH_3 under the conditions used here. Exposure of the NH/Pt(111) surface to D_2 at 380 K produces the ND species. Comparison with the results of density functional theory calculations based on small Pt clusters indicates that NH occupies three-fold hollow sites with the molecular axis perpendicular to the surface.

Introduction

The characterization of species of the form NH_x ($x = 0, 1, 2, 3$) on metal surfaces is important in establishing the reaction mechanisms for a variety of catalytic processes. These include ammonia synthesis from N_2 and H_2, ammonia oxidation, and NO reduction by automotive catalysts. Although platinum is not used for ammonia synthesis, it is used for ammonia oxidation. Also, surface NH_x species play a crucial role in the synthesis of HCN from NH_3 and CH_4 over platinum catalysts. Insights into the surface processes involved have been indirectly inferred by Schmidt and co-workers from extensive studies on the kinetics of HCN formation over Pt and Rh catalysts.[1] In recent work,[2] we have induced C−N coupling on a Pt(111) surface under ultrahigh vacuum conditions from surface carbon and nitrogen atoms produced by electron irradiation of co-adsorbed NH_3 and CH_3I. Here, we explore the properties of NH on Pt(111) that is produced from the electron-induced dissociation of adsorbed ammonia.

The surface properties of NH have been extensively studied on ruthenium surfaces, and the results make for an interesting comparison with the results reported here on Pt(111). Wang and Jacobi[3] found that NH_3 dehydrogenates thermally in a stepwise fashion to NH_2 and NH on Ru(11$\bar{2}$0) and used high-resolution electron energy loss spectroscopy (HREELS) starting with both NH_3 and $^{15}ND_3$ to show that the bending mode of NH on this surface occurs at a rather low value of just below 700 cm^{-1}. Similar results were obtained earlier on Ru(11$\bar{2}$1).[4] Reflection absorption infrared spectroscopy (RAIRS) over the range from 700 to 3700 cm^{-1} for NH/Ru(001)[5] prepared by the forward reaction

$$N + H \rightleftharpoons NH \qquad (1)$$

with the surface N atoms prepared from NO dissociation, showed an intense NH stretch at 3320 cm^{-1}, but no other peaks, establishing that a dipole-active bending mode for NH does not occur above 700 cm^{-1}. This appears to be the only previous RAIRS result for surface NH. Staufer et al.[5] also used density functional theory (DFT) to calculate the vibrational frequencies for NH on Ru(001) and to argue that previous assignments of a peak in the range of 1270−1360 cm^{-1} to the NH bending mode of NH on various surfaces were incorrect. Surface NH has been identified with HREELS from the reaction of chemisorbed N and H atoms on Ru(10$\bar{1}$0)[6] and Ru(001)[7] and on Ru-(001) from the decomposition of hydrazine[8] and formamide.[9] Recently, theoretical rate constants were calculated for the N + H → NH reaction on Ru(001) as a function of temperature.[10]

The existence of a stable NH species on Pt, Rh, Ir, Fe, Ru, and Re surfaces has been predicted on the basis of semiempirical calculations.[11] These calculations indicate that, while NH is stable on all six metals, NH_2 has little stability on Pt, Rh, or Ir. Experimentally, a stable NH species has been detected with HREELS on Ni(111) following hydrazine decomposition[12] and on Ni(110) from ammonia decomposition.[13] When coadsorbed with oxygen, ammonia is found to decompose to yield NH on Cu(110)[14] and Ag(110).[15] An NH_x species produced from the reaction of NO and H_2 was found with HREELS on the Pd-(100),[16] $Pt_{0.25}Rh_{0.75}$(100),[17] and Rh(100)[18] surfaces. Evidence for an NH species was found with HREELS in the reaction of NO with H_2 on the Pt(100) surface.[19] In a study of ammonia oxidation on Pt(111), Mieher and Ho[20] noted that, while less than 3% of the ammonia dissociates on the clean surface, electron beam exposure is very effective in dissociating ammonia to the NH species. They also noted that the NH produced has very strong dipole activity. Later work by Sun et al.[21] focused on the formation and characterization with HREELS of NH_2 and NH on Pt(111) produced through electron-induced dissociation of an adsorbed NH_3 layer. Further details of the electron-induced dissociation of NH_3 on Pt(111) were reported by Bater et al.[22] Our study confirms many of the general features established for NH on metal surfaces in previous studies. However, the higher resolution and rigorous surface selection

* Corresponding author. E-mail: mtrenary@uic.edu.

10.1021/jp046899e CCC: $30.25
Published on Web 01/28/2005

rules available with RAIRS clarify issues raised in the HREELS experiments.

Experimental Section

The experiments were performed in a stainless steel ultrahigh vacuum (UHV) chamber with a base pressure of $\sim 1 \times 10^{-10}$ Torr. A detailed description of this system can be found elsewhere.[23] The UHV chamber is equipped for Auger electron spectroscopy (AES), low energy electron diffraction (LEED), and temperature programmed desorption (TPD) experiments with a quadrupole mass spectrometer (QMS). It is coupled to a commercial Fourier transform infrared (FTIR) spectrometer, a Bruker IFS 66 v/S. The IR beam enters and exits the UHV chamber through differentially pumped O-ring sealed KBr windows and passes through a polarizer before reaching the infrared detector. The spectra in Figures 3 and 4 were obtained at 4 cm^{-1} resolution with an MCT (HgCdTe) detector, whereas the spectra in Figures 6 and 7 were obtained at 2 cm^{-1} resolution with an InSb detector. In cases where the sample was annealed to a temperature above 85 K, the sample was then cooled back to 85 K before the spectrum was acquired. The background reference spectrum was also taken at 85 K. The Pt(111) surface was cleaned by a procedure described earlier.[24] Briefly, the crystal was heated in 1×10^{-7} Torr of O_2 at $\sim$825 K for 1 h after Ar^+ bombardment followed by dosing 2 L (1 L = 1×10^{-6} Torr s) of O_2 at 85 K and subsequently performing a TPD experiment from 85 to 1000 K. The surface was judged free of carbon when a $m/e = 32$ peak at 720 K, due to recombinative desorption of oxygen, was observed in the absence of any CO_2 ($m/e = 44$) desorption above 300 K. The absence of impurities other than carbon was verified with Auger electron spectroscopy. Ammonia (99.9992% pure) and H_2 (99.9999% pure) were obtained from Matheson Tri-Gas, Inc., and D_2 (99.5% pure) was obtained from Union Carbide Corp., Linde Division. All gases were used without further purification. Electron beam exposures were performed with the electron gun included in the LEED apparatus and were defocused to cover as much of the crystal as possible. A total electron exposure of 4.2×10^{15} electrons/cm^2 was used for all experiments reported here. A magnet was moved by hand above the chamber during electron-beam exposures to deflect the beam over the entire surface.

Results

1. Temperature Programmed Desorption. The only desorption products observed with TPD after NH_3 adsorption were NH_3 ($m/e = 17$), H_2 ($m/e = 2$), and N_2 ($m/e = 28$). To distinguish between the desorption of CO ($m/e = 28$) adsorbed from the background and the desorption of N_2 from NH_3 decomposition, we monitored both the $m/e = 28$ and the $m/e = 14$ channels, because the latter is almost entirely due to N atoms from N_2 dissociation in the ionizer of the mass spectrometer. Figure 1 shows TPD results for NH_3 exposures of 0.2 and 1.0 L with and without exposure to a 100 eV electron beam. The NH_3 desorption peak at 111 K for a 1.0 L exposure is due to multilayer desorption and is absent for the 0.2 L case. The latter exposure in the absence of electron irradiation leads to ammonia desorption over a broad temperature range beginning at around 130 K and extending almost to 400 K. This is consistent with previous studies, where the lower temperature peak in the range of 133−186 K is assigned to so-called "β ammonia" and the desorption at higher temperatures is attributed to "α ammonia", with the β form presumably due to a second layer, and the α form corresponding to ammonia molecules directly bonded to the platinum surface. Fisher[25] showed that

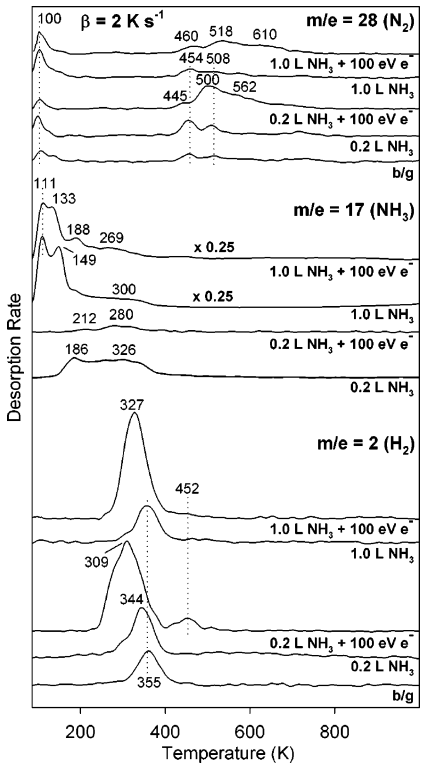

Figure 1. Temperature programmed desorption of H_2, N_2, and NH_3 following 0.2 and 1.0 L exposures of NH_3 to the surface at 85 K with and without exposure to 100 eV electrons.

the α state saturates at a quarter monolayer (3.8×10^{14} cm^{-2}) and that the β-NH_3 can have a coverage that is 2−3 times that in the α state. We follow the same convention as used by Fisher in defining a monolayer coverage as one adsorbate molecule per surface platinum atom, such that one monolayer corresponds to an areal density of 1.50×10^{15} cm^{-2}. It is likely that the β-NH_3 molecules are hydrogen bonded to the α-NH_3, and the combined α and β layers are often referred to as a bilayer. The effect of electron beam exposure is most pronounced for the 0.2 L NH_3 exposure and is seen to eliminate the 186 K NH_3 desorption peak and to decrease the total amount of NH_3 that desorbs molecularly. The fact that electron irradiation leads to ammonia dissociation, as opposed to just electron stimulated desorption, is revealed by the substantial increase in the amount of H_2 and N_2 desorption following electron exposure. The N_2 desorption for 0.2 L NH_3 without electron irradiation shows an increase in the 500 K peak over the background case and is consistent with a small amount of thermal dissociation of ammonia. The fact that the 0.2 L exposure also leads to a slight increase in the 454 K CO peak is likely due to displacement of CO on the chamber walls by NH_3, thus raising the background CO pressure during the experiment. Without electron exposure, there is a small increase in the amount of H_2 that desorbs relative to the background trace, and like the increase in N_2 desorption noted above, this increase is attributed to a small amount of thermal dissociation of ammonia. In addition to the increased amount of H_2 desorption in the 300−360 K range, electron irradiation following 0.2 L of NH_3 leads to a distinct peak at 452 K, which is largely absent for 1.0 L of ammonia.

Although substantially more ammonia is on the surface for the 1.0 L exposure than for the 0.2 L case, the total amount of the dissociation products, H_2 and N_2, is not much different. There are two possible explanations of this. First, the second and higher layers of ammonia may shield the monolayer from the effects of the electron beam. At the same time, electron

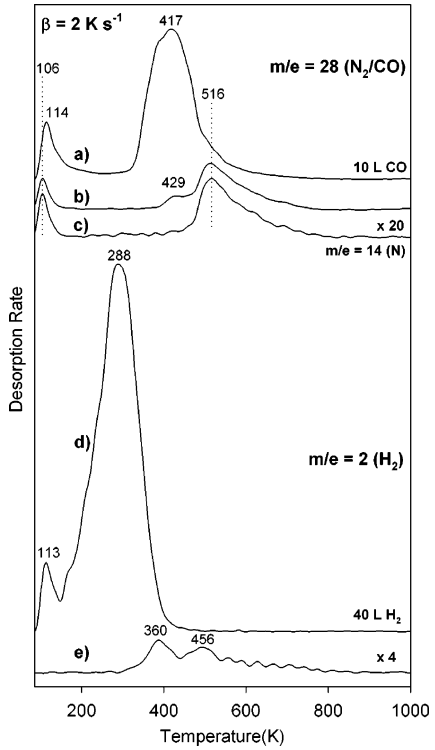

Figure 2. Temperature programmed desorption of H_2 (e) and N_2 (b) and (c) following a 0.4 L exposure to NH_3 at 85 K and exposure to 100 eV electrons as compared to saturation coverages of CO (a) and H_2 (d) on the clean surface. In (e), the surface was annealed to 380 K for 30 s and cooled back to 85 K before the TPD experiment.

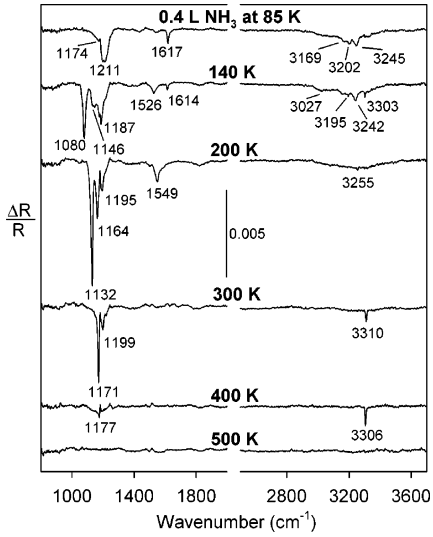

Figure 3. RAIR spectra following a 0.4 L exposure to ammonia at 85 K and annealing to the indicated temperatures.

stimulated desorption of the ammonia occurs, which will remove the multilayers thus exposing the monolayer to electron irradiation and hence dissociation. Second, platinum surface sites that are needed to stabilize the dissociation products may be unavailable at higher ammonia coverages. Both explanations are consistent with the fact that the amount of H_2 desorption is about the same even though the NH_3 coverages differ by a factor of 5.

Further information on the dissociation of the NH species is provided by the TPD results shown in Figure 2, which were obtained following a 0.4 L ammonia exposure at 85 K, electron irradiation, annealing to 380 K to desorb excess hydrogen and to convert as much surface nitrogen to NH as possible, and cooling back to 85 K. Also shown for comparison are TPD traces (a) and (d) for saturation coverages of CO and H for CO and H_2 exposures at 85 K. Comparison of the $m/e = 28$ and $m/e = 14$ traces in (b) and (c) shows that the desorption in (b) at 516 K is due to N_2, whereas the shoulder at 429 K is due to CO. Bater et al.[22] obtained a similar result and showed that the peak shifted to lower temperatures with increasing electron exposure, implying second-order kinetics, as expected for recombinative desorption of N_2. The H_2 result (e) was obtained after annealing the electron irradiated ammonia layer to 380 K for 30 s to desorb as much hydrogen as possible that is not associated with the NH species.

2. Reflection Absorption Infrared Spectroscopy. The behavior of the RAIR spectra in the absence of electron irradiation is shown in Figure 3 for a 0.4 L exposure. Thermal desorption results for NH_3 as a function of NH_3 exposure (not shown here) indicate that a 0.4 L exposure just saturates the β state. The spectra in Figure 3 thus correspond to NH_3 molecules bonded directly to the surface as well as second layer molecules. Although the spectra are complex, they are generally consistent with previous vibrational studies of the NH_3/Pt(111) system using HREELS[20,21,26] and RAIRS.[27] Villegas and Weaver[27] proposed that there is a hydrogen-bonding interaction between the nitrogen atoms of the β-NH_3 with the hydrogen atoms of the α-NH_3 and that the α and β forms coexist well before the first layer is complete. Because of the hydrogen bonding and other types of adsorbate−adsorbate interaction, the vibrational frequencies are highly sensitive to the local environment of a given ammonia molecule. Thus, each mode displays a wide range of frequencies. The peaks in the range of 1080−1199 cm^{-1} correspond to the symmetric NH_3 deformation, peaks in the range of 1526−1617 cm^{-1} are due to the asymmetric deformation, and the complex set of peaks in the 3150−3250 cm^{-1} region are due to both symmetric and asymmetric NH stretch peaks. If chemisorbed ammonia is simply bonded to an on-top site through the nitrogen lone pair of electrons, one would expect the C_3 molecular axis to be perpendicular to the surface, giving a local symmetry of C_{3v}. In such a case, the $\delta_{as}(NH_3)$ and $\nu_{as}(NH)$ modes would not be dipole allowed and would not be observed at all with RAIRS. The selection rules are less clear-cut with HREELS, and Sexton and Mitchell[26] took considerable care to determine whether the observed modes were dipole excited or excited by impact scattering. The appearance of the 1617 cm^{-1} peak in Figure 3 immediately after adsorption at 85 K shows that at least some of the molecules are oriented with the C_3 axis tilted with respect to the surface normal. Annealing the surface to 300 K eliminates all ammonia peaks except those assigned to $\delta_s(NH_3)$, and because only α-NH_3 should remain on the surface at 300 K, it follows that the α-NH_3 molecules are oriented with their axes perpendicular to the surface under these conditions.

Annealing the adsorbed NH_3 bilayer to higher temperatures causes pronounced changes in the spectra. The 140 K anneal leads to a broader distribution of ammonia peaks, and by 200 K the NH stretch region is a broad and essentially structureless envelope centered at 3255 cm^{-1}. The 200 K anneal also causes the $\delta_{as}(NH_3)$ peak to shift to 1549 cm^{-1} and the $\delta_s(NH_3)$ mode to split into three components at 1132, 1164, and 1195 cm^{-1}. The TPD results for a 0.4 L exposure (not shown) indicate that both the 140 and the 200 K anneals should cause desorption of ammonia molecules. However, there is no evidence, in our work or that of others, that these anneals result in dissociation of ammonia so that the range of features seen in the top three

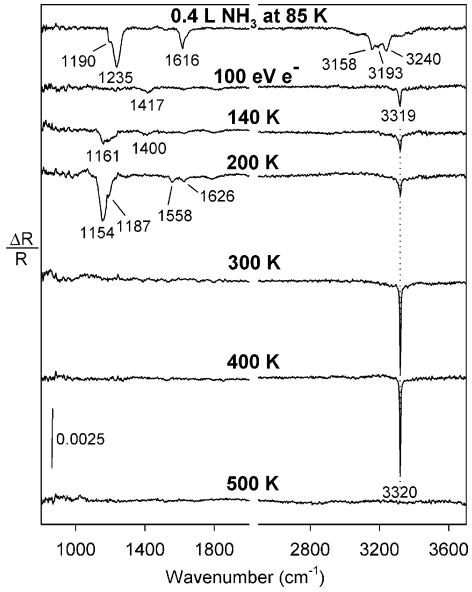

Figure 4. RAIRS of 0.4 L of NH_3 at 85 K, followed by exposure to 100 eV electrons and annealing to the indicated temperatures.

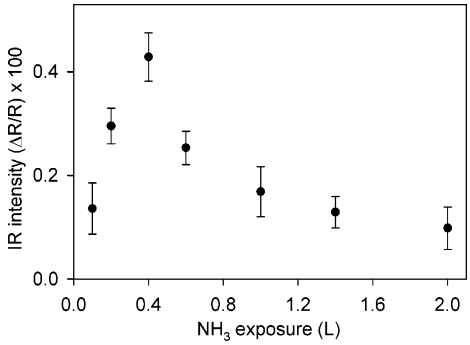

Figure 5. Plot of the NH stretch intensity of NH as a function of NH_3 exposure.

spectra of Figure 3 reflect structural changes in an adsorbed layer of intact but fewer NH_3 molecules. However, with the 300 K anneal, a new peak appears at 3310 cm^{-1} due to the NH species. This peak is only slightly shifted to 3306 cm^{-1} with the 400 K anneal, which desorbs most of the remaining ammonia. The observation of NH on the surface demonstrates that even in the absence of electron irradiation there is a small amount of thermal decomposition of ammonia on Pt(111). The same result was obtained in a separate experiment with the sample biased to −200 V, demonstrating that the dissociation was not induced by stray electrons from the ion gauge. Comparison of results for 0.4 and 1.0 L exposures reveals that the higher exposure leads to less NH, suggesting the blocking of reactive sites at higher coverages. An earlier study using molecular beams of NH_3 scattered from the flat Pt(111) and stepped Pt(557) surfaces[28] indicated a dissociative sticking probability that is 16 times higher on the stepped surface. This suggests that the reactive sites in our case are also the step sites.

The transformation of the ammonia layer in response to irradiation with 100 eV electrons is revealed by the RAIRS results in Figure 4. Variation of the beam energy indicated that 100 eV gives the maximum coverage of the NH product. The electron irradiation at 85 K causes all of the features attributed to ammonia to greatly diminish, and the resulting spectrum has a single sharp peak at 3319 cm^{-1} and a weak peak at 1417 cm^{-1}. Upon annealing the surface to 140 K, a peak at 1161 cm^{-1} appears. As Sexton and Mitchell[26] have shown, annealing a low coverage of ammonia results in a strong increase in the symmetric NH_3 deformation mode, accompanied by a decrease in intensity of the other ammonia modes. The reappearance of the ammonia modes following annealing to 140 and 200 K is most likely due to reordering of residual ammonia left on the surface as observed in Figure 3. The fact that the 3319 cm^{-1} peak of NH does not diminish in intensity as the ammonia peaks grow in with the 140 and 200 K anneals in Figure 4 indicates that NH_3 is not produced by hydrogenation of NH.

The most significant changes observed in Figure 4 occur after annealing to temperatures of 300, 400, and 500 K. The 300 K anneal eliminates the ammonia peaks and results in a sharp increase in the intensity of the 3320 cm^{-1} peak. From the value of the frequency, and the absence of other peaks in the spectrum, this peak is assigned to the NH species. Staufer et al.[5] have summarized the N−H stretch frequencies reported in previous HREELS studies of NH on metal surfaces, which range from 3150 to 3315 cm^{-1}. In their HREELS study of NH on Pt(111), Sun et al.[21] reported the NH stretch at 3281 cm^{-1}. The earlier RAIRS spectrum of Staufer et al.[5] for NH on Ru(001) showed a completely featureless spectrum except for a sharp and intense peak also at 3320 cm^{-1}. The large increase of the N−H stretch upon heating from 200 to 300 K shows that reaction 1 occurs in that temperature range. In the study by Sun et al.,[21] there is no indication that once N and H atoms are produced on Pt(111) they can recombine to form NH. On Ru(001), Shi et al.[7] found that surface N could be hydrogenated only by exposure to H_2 at 300 K, but not by annealing a H and N covered surface from low temperatures. Thus, reaction 1 appears to be particularly facile on Pt(111). There is little change in the spectra between 300 and 400 K, but the 500 K anneal dissociates the NH leading to the elimination of the ν(NH) peak.

The H_2 thermal desorption results in Figure 1 showing that the 452 K peak attributed to NH dissociation was larger for a lower NH_3 coverage implied that the maximum NH coverage occurs at relatively low NH_3 exposures. This is confirmed by the plot of RAIRS NH stretch intensity as a function of ammonia exposure in Figure 5, which shows a maximum at 0.4 L. Similarly, a maximum is also obtained at 0.4 L in a plot (not shown) of the area of the H_2 TPD peak at 450 K versus NH_3 exposure. The conditions thus established for achieving the maximum NH coverage, at least within the set of parameters considered here, were then used to further characterize the NH species.

The results shown in Figure 6 relate to both the forward and the reverse directions of reaction 1. The topmost spectrum shows a sharp and intense ν(NH) peak at 3321 cm^{-1} with a measured FWHM of 4.8 cm^{-1} at the maximum NH coverage. There is a clear shoulder on this peak at about 3310 cm^{-1}. The next spectrum was obtained following heating to 420 K for 30 min. These conditions were chosen to dissociate the NH while minimizing the amount of N_2 desorption. The remaining NH peak at 3312 cm^{-1} has only 16% of the area of the initial peak and is broadened to 11.2 cm^{-1}. A 20 L H_2 exposure partially restores the NH peak area to 78% of its initial value, but the position and width of the peak are similar to their values after the 420 K anneal. As the bottom two spectra show, additional H_2 exposures do not increase the peak area but lead to a slight increase in the FWHM. By exposing to hydrogen at 380 K, the excess hydrogen that does not react to form NH desorbs as H_2.

The extent to which ND can be formed from NH through exchange is shown in Figure 7. The initial spectrum was obtained in the same way as in Figure 6a and shows the main peak at 3321 cm^{-1}, with a small satellite peak at 3309 cm^{-1}

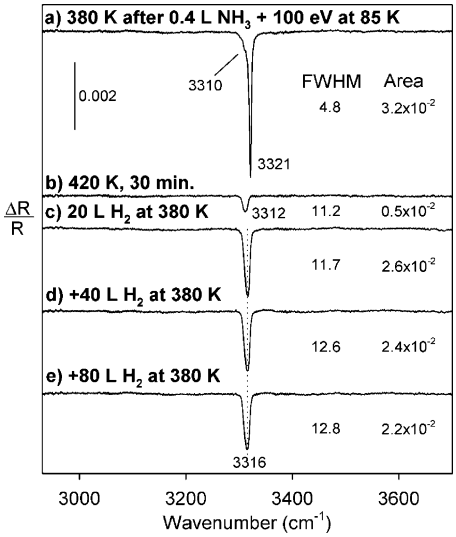

Figure 6. RAIR spectra obtained with a resolution of 2 cm^{-1} showing dissociation and reformation of the NH species: (a) after a 0.4 L NH_3 exposure at 85 K, irradiation with 100 eV electrons, annealing to 380 K, and cooling back to 85 K; (b) after heating the surface in (a) to 420 K for 30 min and cooling back to 85 K; (c) after heating the surface in (b) to 380 K, exposure to 20 L of H_2 at 380 K, and cooling back to 85 K; (d) after heating the surface in (c) to 380 K, exposure to an additional 40 L of H_2 at 380 K, and cooling back to 85 K; and (e) after heating the surface in (d) to 380 K, exposure to an additional 80 L of H_2 at 380 K, and cooling back to 85 K.

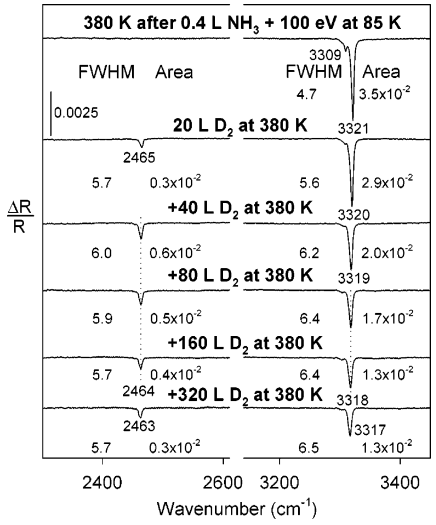

Figure 7. RAIR spectra obtained with a resolution of 2 cm^{-1} showing the extent of D exchange in NH. The NH species was prepared after a 0.4 L NH_3 exposure at 85 K, irradiation with 100 eV electrons, annealing to 380 K, and cooling back to 85 K. In each of the subsequent spectra, the surface was exposed to the indicated amount of D_2 and cooled back to 85 K where the spectra were recorded.

corresponding to the unresolved shoulder at about 3310 cm^{-1} in Figure 6a. After a 20 L D_2 exposure at 380 K, an ND stretch appears at 2465 cm^{-1} and the NH stretch has decreased by 17% in area and has become slightly broader. An additional 40 L D_2 exposure (for a total of 60 L) doubles the ND area, but subsequent D_2 exposures have no effect and the longer times involved lead to a gradual loss of combined ND + NH intensity. Although other compelling evidence already described indicates that the species on the surface under these conditions is NH (or ND), the fact that only one additional peak is produced upon D_2 exposure further supports this assignment because an NH_2 species would exchange to give NHD and ND_2, resulting in an additional peak, which is not seen. The results in Figure 7 clearly show that only some of the NH initially present can undergo deuterium exchange to form ND. This is similar to the results in Figure 6 showing that only some of the surface N present on the surface can be rehydrogenated to form NH.

Another factor leading to the relatively weak ND stretch is that the RAIRS intensity per unit coverage for NH is higher than that for ND. If the initial NH coverage is designated θ_{NH}, and the NH and ND coverages after exchange as θ'_{NH} and θ_{ND}, then it is reasonable to assume that $\theta_{NH} = \theta'_{NH} + \theta_{ND}$, and that $\theta'_{NH}/\theta_{NH} = A'_{NH}/A_{NH}$, where the latter is the ratio of the NH peak area after exchange to the area before exchange. As noted above, this assumption is not valid for the longer times associated with the higher D_2 exposures used in Figure 7, but we will assume that it holds at least approximately for the first 20 L D_2 exposure, in which case it then follows that the intensity ratio per molecule is given by $I_{NH}/I_{ND} = (A_{NH} - A'_{NH})/A_{ND} = 0.6/0.3 = 2.0$. The DFT calculations predict that the intensity for NH should be greater than that for ND by a factor of 1.87, which is the square of the frequency ratio. The calculated intensity ratio is not an electronic structure effect as the dipole derivatives with respect to internal coordinate should be the same for the NH and ND stretches, but the calculated intensities depend on dipole derivatives with respect to normal coordinates, and normal coordinates are defined to contain a mass factor. Thus, the observed relative intensities for NH and ND are about what would be expected.

Table 1 shows the results of DFT calculations for NH at on-top, two-fold bridge, and hcp three-fold hollow sites based on cluster models. The on-top site was modeled by both a single Pt atom and a planar array of seven Pt atoms. The two-fold bridge site was modeled by two Pt atoms, and the three-fold hollow site was modeled by a cluster consisting of a triangle of Pt atoms with a single Pt atom located below the center of the triangle. Figure 8 shows the optimized geometries for NH attached to the Pt_4 and Pt_7 cluster models. Similar models were used in ref 5 to represent NH on the Ru(001) surface. Our calculations were carried out using the Gaussian 98 code[29] with the B3LYP functional[30] and a split valence, d−p polarization function 6-311G** basis set for N and H. The Hay−Wadt semi-relativistic pseudopotential[31] was used to represent the core electrons of Pt. The associated basis set was also used for the description of the Pt valence electrons. The Pt−Pt distance was kept fixed at a distance of 2.775 Å, and the other geometrical parameters were optimized in the calculations. However, for NH on the Pt_7 cluster, the N atom position was fixed above the central Pt atom as the optimized geometry would place it at the adjacent three-fold hollow site. The frequencies given here have been scaled by a factor of 0.9613. The results show that the value of ν(NH) is quite sensitive to adsorption site and that the experimental values, which range from 3304 to 3321 cm^{-1} depending on coverage, are only consistent with adsorption at the three-fold hollow site. Geometry optimization of the Pt_4−NH cluster gives an angle of less than 7° between the NH bond and the normal to the plane of the three Pt atoms to which the N atom is bonded. For NH on the Pt_7 cluster, the optimized geometry gives a bent PtNH unit with an angle of 74° from the normal of the Pt_7 plane. Staufer et al.[5] also calculated a bent NH for the on-top site of their planar Ru_7 cluster. Furthermore, they provide an extensive discussion of the electronic structure of various X−NH species in the context of considering the bending mode frequency. They note that while the CNH species is linear, ONH is bent, which they explain is due to the placement of the extra pair of electrons into an orbital that

TABLE 1: Calculated Frequencies and IR Intensities (I) for NH (ND) for Cluster Models of Bonding at On-Top (Pt−NH, Pt_7−NH)), Two-Fold Bridge (Pt_2−NH), and Three-Fold Hollow Sites (Pt_4−NH)

	Pt−NH		Pt_7−NH		Pt_2−NH		Pt_4−NH		exp
mode	cm^{-1}	I	cm^{-1}	I	cm^{-1}	I	cm^{-1}	I	cm^{-1}
ν (Pt−NH)	811	5.5	698	6.0	585	24.5	547	0.31	488[a]
δ (NH)	978	65.6	1034	80.4	862	35.0	669	2.9	
ν (NH)	3082	1.9	3122	4.3	3163	6.1	3329 (2434)	67.3 (36.0)	3320 (2464)

[a] From the HREELS study of ref 21.

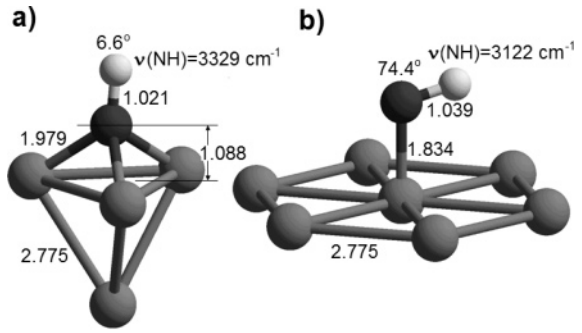

Figure 8. Optimized geometries obtained from the DFT calculations for NH attached to (a) a Pt_4 model of a three-fold hollow site and (b) a Pt_7 model of an on-top site. In both cases, the Pt−Pt distances were fixed at 2.775 Å. In (b), the N atom position was fixed above the central Pt atom.

changes to lower energy as the molecule is bent. Thus, it would appear that NH at an atop site on a metal surface resembles ONH and NH at the three-fold hollow site resembles CNH. For the on-top site of the Pt_7 model, the most intense peak is predicted to be the PtNH bend at 1034 cm^{-1}, a value well above the low wavenumber cutoff of our detector. The fact that a peak in this region is not observed, whereas a strong peak is observed for the NH stretch, makes this model incompatible with the experimental result. The ν(Pt−NH) mode for NH on Pt(111) was reported at 488 cm^{-1} in the HREELS study of Sun et al.,[21] but they did not report a bending mode for NH. Staufer et al.[5] also concluded that NH occupies a three-fold hollow site on Ru(001) with the NH bond perpendicular to the surface.

Discussion

The focus of this study is the characterization of NH and its reversible formation from surface N and H atoms as represented by reaction 1. Intriguing issues that we do not address further are the structure of the chemisorbed ammonia layer or the detailed mechanism by which NH_3 is converted to surface N and H and whether the conversion occurs stepwise through NH_2 and NH intermediates. Sun et al.[21] provided some HREELS data for NH_2 on Pt(111) produced through exposure to a 50 eV electron beam. We have also obtained data using 50 eV electrons, but the results are complicated by the fact that NH_2 does not appear to be stable enough to survive the annealing needed to desorb residual ammonia so that there is ambiguity as to whether the observed peaks are due to NH_3 or to NH_2. This makes it difficult to definitively characterize NH_2 with RAIRS and to determine its role in the overall reaction chemistry. Similarly, the presence of the NH species as revealed by the weak peak at 3319 cm^{-1} in Figure 4 after a 100 eV electron exposure at 85 K but before annealing indicates that NH can be produced directly from the loss of two H atoms from NH_3 because the thermal reaction to produce NH by reaction 1 does not take place until 200 K. However, it is not clear why higher coverages of NH cannot be produced by this route.

The characterization of NH is made easier by the fact that it is stable to a relatively high temperature and because its N−H stretch mode has high intensity. Under the conditions where it is most intense, this peak has a $\Delta R/R$ value of 0.004. This can be compared to the symmetric CH stretch of ethylidyne (CCH_3) at 2887 cm^{-1}, which we have measured with 4 cm^{-1} resolution to have a $\Delta R/R$ value of 0.0014 at a coverage of 0.25 ML.[32] A more meaningful comparison requires knowledge of the absolute NH coverage, which can be obtained from TPD in two different ways. First, we find that the absolute N atom coverage is 0.27 ML for the NH coverage that gives the maximum RAIRS intensity. This determination is based on a saturation coverage for CO of 0.68 ML[33] and on the fact that the mass spectrometer has almost the same sensitivity for CO and N_2. If all of the N is associated with NH under the conditions of Figure 2, then the NH coverage is also 0.27 ML. Second, the NH coverage can be obtained from a comparison of the area of the 456 K H_2 peak in Figure 2e with the H_2 peak for a saturation coverage of hydrogen on Pt(111) (Figure 2d), which is known to be 1.0 ML.[34] This implies a much lower NH coverage of only 0.02 ML, indicating that only a small fraction of the N atoms on the surface can be hydrogenated to form NH. An NH coverage of 0.27 would imply that, per unit coverage, the N−H stretch is about 2.7 times as intense as the C−H stretch of ethylidyne. However, if we take the NH coverage as 0.02 ML, then the N−H stretch has an intrinsic intensity that is 36 times the intensity of the C−H stretch of ethylidyne. Because vibrational intensities are highly variable, the intensity of the N−H stretch provides no basis for estimating the NH coverage or for questioning the implication of the TPD results that at the maximum NH coverage the surface contains a high N to NH ratio.

The idea that NH coexists with a much larger number of unreactive N atoms provides a basis for interpreting the RAIRS results in Figures 6 and 7. At the maximum NH coverage achieved here, the NH stretch frequency is 3321 cm^{-1}, while at the lowest NH coverages it occurs at 3304 cm^{-1}. The shift to higher frequencies for the internal stretch mode of a diatomic adsorbate oriented perpendicular to a surface is consistent with a dipole−dipole interaction.[35] In addition to the main peaks at 3320−3321 cm^{-1} for the initial spectra in Figures 6 and 7, there are much less intense lower wavenumber components at 3309−3311 cm^{-1}. We assume that the main high frequency peak corresponds to molecules in dense islands of NH or of NH and N atoms and the lower frequency components correspond to NH molecules that are part of a less dense phase between NH islands or at the island perimeters. It then follows that deuterium atoms are able to exchange readily with NH outside of ordered islands, or at island edges, which would explain our inability to convert all of the NH to ND. The results in Figure 7 reveal that the low-frequency component at 3309 cm^{-1} disappears upon the first D_2 exposure. In other results that are not shown here, it is found that at much lower NH coverages a higher fraction of the NH can be converted to ND by D_2 exposure. In the results for NH dissociation and reformation in Figure 6, the

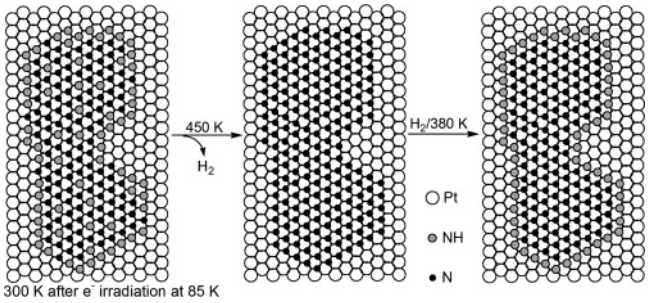

Figure 9. An assumed island structure model showing NH initially at both the perimeter and the interior sites of a 1×1 N atom island, which is converted to an N atom island of the same structure after NH dehydrogenation. Rehydrogenation is shown to produce NH only at the island perimeter, which would account for the experimental observation that at the maximum NH coverage, not all of the initial NH can be reformed by exposure to H_2.

reformed NH has a lower frequency, a larger line width, and a reduced peak area as compared to the initial NH. This suggests that dense islands of adsorbed nitrogen atoms are formed from the dense NH islands and that adsorbed H atoms cannot penetrate into the interior of these islands to reform NH. This then limits the amount of NH that can be formed from reaction 1 both under the conditions of Figure 6 as well as by annealing the electron irradiated layer as in Figure 4. A likely reason that a higher NH coverage can be achieved under the conditions of Figure 4 than can be achieved by rehydrogenating surface N atoms is that ordering of the N atoms into dense islands is a thermally activated process so that for the N atoms produced from NH_3 dissociation at 85 K, a greater fraction is initially in a less dense phase, which facilitates their reaction with H atoms. This could also explain why there is a gradual loss of combined NH + ND intensity with longer times at 380 K in Figure 7, which is presumably due to the conversion of surface nitrogen into an unreactive form in the interior of islands. The idea that dense islands of NH are converted into dense islands of N atoms, which can only be rehydrogenated around the island perimeter, is illustrated in Figure 9. In the initial overlayer, the NH is drawn occupying both the island perimeter and being distributed among adsorbed N atoms in the island interior. For simplicity, N atoms and NH molecules outside of the island are not shown, although they must surely be present. One observation that reveals that Figure 9 is an oversimplification is the larger NH stretch line width for the rehydrogenated NH, as observed in Figure 6, suggesting that it has a more heterogeneous environment than the initial NH. In contrast, in Figure 9 the rehydrogenated NH is shown as occurring in only one environment, at the perimeter of regular-shaped islands, whereas the initial NH is shown as being present at both the perimeter and the interior of the island. This indicates that the actual island structure is more complicated than drawn. For example, if the islands have an irregular shape, then there would be a greater heterogeneity in the environment of the perimeter molecules. Hydrogen exposure may also cause large N atom islands to break-up into smaller islands with a wide distribution of sizes and shapes. The idea that reaction 1 occurs only around the perimeter of N islands was also invoked to explain the kinetics of NH formation from $c(2 \times 2)$ islands of N atoms on the Pd(100),[16] $Pt_{0.25}Rh_{0.75}(100)$,[17] and Rh(100)[18] surfaces, where it was also found that only a small fraction of the surface N could be converted to NH_x. Although x was not identified in these studies,[16−18] the present work strongly implies that the species was in fact NH.

Summary

Electron-induced dissociation of NH_3 on the Pt(111) surface has been used to produce a mixed NH + N layer. The NH species is characterized with RAIRS to have an unusually strong N−H stretch mode with a fairly narrow line width, which enables the detection of NH over a wide coverage range. Comparison of the experimental results with the results of density functional theory calculations indicates that the NH adsorbs at three-fold hollow sites with the NH axis aligned close to the surface normal. The N−H bond of NH breaks upon heating to 450 K, but the nitrogen atoms produced can be rehydrogenated by additional exposure to H_2 at 380 K. The high reactivity of surface N atoms toward hydrogen was not established in previous studies on Pt(111) and appears to be higher than observed on Ru surfaces. However, unlike Ru, the hydrogenation reaction does not proceed beyond NH to form NH_2 or NH_3 on Pt(111). Although we find that surface NH is readily formed upon hydrogen exposure to the adsorbed N layer, H_2 TPD results indicate that many of the adsorbed N atoms are in an unreactive form and cannot be converted to NH. An island model is proposed in which only N atoms on the island perimeters are able to react with hydrogen, whereas the N atoms in the island interior are assumed to be unreactive.

Acknowledgment. This work was supported by a grant from the National Science Foundation (CHE-0135561).

References and Notes

(1) Hasenberg, H.; Schmidt, L. D. *J. Catal.* **1986**, *97*, 156. Hasenberg, H.; Schmidt, L. D. *J. Catal.* **1985**, *91*, 116. Schmidt, L. D.; Hickman, D. A. In *Catalysis of Organic Reactions*; Kosak, J. R., Johnson, T. A., Eds.; Marcel Dekker: New York, 1994; pp 195−212.
(2) Herceg, E.; Trenary, M. *J. Am. Chem. Soc.* **2003**, *125*, 15758.
(3) Wang, Y.; Jacobi, K. *Surf. Sci.* **2002**, *513*, 83.
(4) Jacobi, K.; Wang, Y.; Fan, C. Y.; Dietrich, H. *J. Chem. Phys.* **2001**, *115*, 4306.
(5) Staufer, M.; Neyman, K. M.; Jacob, P.; Menzel, D.; Nasluzov, V. A.; Rösch, N. *Surf. Sci.* **1996**, *369*, 300.
(6) Dietrich, H.; Jacobi, K.; Ertl, G. *J. Chem. Phys.* **1997**, *106*, 9313.
(7) Shi, H.; Jacobi, K.; Ertl, G. *J. Chem. Phys.* **1995**, *102*, 1432.
(8) Rauscher, H.; Kostov, K. L.; Menzel, D. *Chem. Phys.* **1993**, *177*, 473.
(9) Parmeter, J. E.; Schwalke, U.; Weinberg, W. H. *J. Am. Chem. Soc.* **1988**, *110*, 53.
(10) Volpi, A.; Clary, D. C. *J. Phys. Chem. B* **2004**, *108*, 336.
(11) Cholach, A. R.; Bulgakov, N. N.; Nieuwenhuys, B. E. *Catal. Lett.* **2003**, *86*, 9.
(12) Gland, J. L.; Fisher, G. B.; Mitchell, G. E. *Chem. Phys. Lett.* **1985**, *119*, 89.
(13) Bassignana, I. C.; Wageman, K.; Küppers, K.; Ertl, G. *Surf. Sci.* **1986**, *175*, 22.
(14) Afsin, B.; Davies, P. R.; Pashusky, A.; Roberts, M. W.; Vincent, D. *Surf. Sci.* **1993**, *284*, 109.
(15) Thornburg, D. M.; Madix, R. J. *Surf. Sci.* **1989**, *220*, 268.
(16) Yamada, T.; Tanaka, K. *J. Am. Chem. Soc.* **1989**, *111*, 6880.
(17) Yamada, T.; Hirano, H.; Tanaka, K.; Siera, J.; Nieuwenhuys, B. E. *Surf. Sci.* **1990**, *226*, 1.
(18) Yamada, T.; Tanaka, K. *J. Am. Chem. Soc.* **1991**, *113*, 1173.
(19) Zemlyanov, D. Y.; Smirnov, M. Y.; Gorodetskii, V. V.; Block, J. H. *Surf. Sci.* **1995**, *329*, 61.
(20) Mieher, W. D.; Ho, W. *Surf. Sci.* **1995**, *322*, 151.
(21) Sun, Y.-M.; Sloan, D.; Ihm, H.; White, J. M. *J. Vac. Sci. Technol., A* **1996**, *14*, 1516.
(22) Bater, C.; Campbell, J. H.; Craig, J. H., Jr. *Surf. Inter. Anal.* **1998**, *26*, 97; *Thin Solid Films* **1999**, *340*, 7.
(23) Brubaker, M. E.; Trenary, M. *J. Chem. Phys.* **1986**, *85*, 6100.
(24) Jentz, D.; Celio, H.; Mills, P.; Trenary, M. *Surf. Sci.* **1995**, *341*, 1.
(25) Fisher, G. B. *Chem. Phys. Lett.* **1981**, *79*, 452.
(26) Sexton, B. A.; Mitchell, G. E. *Surf. Sci.* **1980**, *99*, 523; *Surf. Sci.* **1980**, *99*, 539.
(27) Villegas, I.; Weaver, M. J. *Surf. Sci.* **1996**, *367*, 162.

(28) Guthrie, W. L.; Sokol, J. D.; Somorjai, G. A. *Surf. Sci.* **1981**, *109*, 390.

(29) Frisch, M. J.; Trucks, G. W.; Schlegel, H. B.; Scuseria, G. E.; Robb, M. A.; Cheeseman, J. R.; Zakrzewski, V. G.; Montgomery, J. A., Jr.; Stratmann, R. E.; Burant, J. C.; Dapprich, S.; Millam, J. M.; Daniels, A. D.; Kudin, K. N.; Strain, M. C.; Farkas, O.; Tomasi, J.; Barone, V.; Cossi, M.; Cammi, R.; Mennucci, B.; Pomelli, C.; Adamo, C.; Clifford, S.; Ochterski, J.; Petersson, G. A.; Ayala, P. Y.; Cui, Q.; Morokuma, K.; Malick, D. K.; Rabuck, A. D.; Raghavachari, K.; Foresman, J. B.; Cioslowski, J.; Ortiz, J. V.; Stefanov, B. B.; Liu, G.; Liashenko, A.; Piskorz, P.; Komaromi, I.; Gomperts, R.; Martin, R. L.; Fox, D. J.; Keith, T.; Al-Laham, M. A.; Peng, C. Y.; Nanayakkara, A.; Gonzalez, C.; Challacombe, M.; Gill, P. M. W.; Johnson, B. G.; Chen, W.; Wong, M. W.; Andres, J. L.; Head-Gordon, M.; Replogle, E. S.; Pople, J. A. *Gaussian 98*, revision A.11.3; Gaussian, Inc.: Pittsburgh, PA, 2002.

(30) Becke, A. D. *J. Chem. Phys.* **1993**, *98*, 5648. Hohenberg, P.; Kohn, W.; *Phys. Rev. B* **1964**, *136*, 864. Becke, A. D. *Phys. Rev. A* **1988**, *38*, 3098. Vosko, S. H.; Wilk, L.; Nusair, M. *Can. J. Phys.* **1980**, *58*, 1200. Lee, C.; Yang, W.; Parr, R. G. *Phys. Rev. B* **1988**, *37*, 785. Miehlich, B.; Savin, A.; Stoll, H.; Preuss, H. *Chem. Phys. Lett.* **1989**, *157*, 200.

(31) Hay, P. J.; Wadt, W. R. *J. Chem. Phys.* **1985**, *82*, 299.

(32) Malik, I. J.; Brubaker, M. E.; Moshin, S. B.; Trenary, M. *J. Chem. Phys.* **1987**, *87*, 5554.

(33) Ertl, G.; Neumann, M.; Streit, K. M. *Surf. Sci.* **1977**, *64*, 393.

(34) Christmann, K.; Ertl, G.; Pignet, T. *Surf. Sci.* **1976**, *54*, 365.

(35) Hollins, P.; Pritchard, J. *Prog. Surf. Sci.* **1985**, *19*, 275.